RSC Advances

PAPER

View Article Online
View Journal | View Issue

Cite this: *RSC Adv.*, 2025, **15**, 39391

Multifunctional bioactivity of marine-derived exopolysaccharide EPSR5 from *Kocuria* sp. AG5: insights into structural and broad-spectrum biomedical applications

Mazen M. Ghaith, [a] Riyad A. Almaimani, [b] Ahmed Ghareeb, [c] Mahmoud M. Habibullah, [d] Sozan M. Abdelkhalig, [el] Hanan AlOmari, [f] Faisal Miqad K. Albaqami, [g] Fawzyah Obeedallah Albaldi, [h] Sarah Ayman Alnumaani, [i] Samar Zuhair Alshawwa, [j] Amal Abdullah Alrashidi [j] and Hanaa F. Abd El-Kareem *[k]

Marine bacteria are a valuable source of bioactive polysaccharides with therapeutic potential. In our previous study, we identified an exopolysaccharide produced by *Kocuria* sp. strain AG5 (EPSR5) isolated from the Red Sea, and demonstrated that it is a high-molecular weight, acidic heteropolysaccharide rich in sulfate (25.6%) and uronic acid (21.77%) groups. In the current study, we expanded the structural characterization and biological evaluation of EPSR5. GC–MS and HPLC analyses revealed glucose as the major monosaccharide, accompanied by xylose, arabinose, and glucuronic acid, confirming its heteropolysaccharide and polyanionic character. Thermal analysis (TGA) demonstrated stability up to 257 °C, while SEM–EDX revealed a porous, flake-like morphology enriched in oxygen, sodium, and phosphorus, suggesting phosphorylation and ionic associations. The biological activity of EPSR5 was assessed through a range of pharmacological assays. Antimicrobial testing against seven pathogenic microbes, including two fungal strains (*Candida albicans*, *Mucor circinelloides*), two Gram-positive bacteria (*Enterococcus faecalis*, *Staphylococcus aureus*), and three Gram-negative bacteria (*Escherichia coli*, *Salmonella typhi*, *Helicobacter pylori*), demonstrated potent inhibitory effects. EPSR5 showed notable inhibition zones up to 30 mm against *E. faecalis* and 27 mm against *H. pylori*, with MIC/MBC values as low as 7.8/15.62 μg mL^{-1} and 15.62/15.62 μg mL^{-1}, respectively. Significant antibiofilm activity was also observed, with inhibition rates reaching up to 96.54% against *E. faecalis* and 97.39% against *H. pylori*, in a concentration-dependent manner. Antioxidant potential was confirmed *via* TAC and FRAP assays, showing values of 62.8 ± 0.3 and 114.9 ± 0.5 μg ascorbic acid equivalents per mg, respectively. EPSR5 exhibited antidiabetic activity by inhibiting α-glucosidase and α-amylase enzymes with IC_{50} values of 17.06 μg mL^{-1} and 66.35 μg mL^{-1}, respectively, comparable to Acarbose. Additionally, EPSR5 inhibited pancreatic lipase with an IC_{50} of 41.39 μg mL^{-1} and suppressed 90.1% of enzyme activity at 1000 μg mL^{-1}. In wound healing assays, EPSR5 promoted fibroblast migration and accelerated wound closure, reducing the wound area within 48 hours, achieving 71.85% closure compared to 66.24% in control cells. Overall, these findings suggest that EPSR5 from *Kocuria* sp. AG5 exhibits multifaceted bioactivities with promising therapeutic potential for antimicrobial, antioxidant, antidiabetic, and wound healing applications.

Received 4th June 2025
Accepted 29th September 2025

DOI: 10.1039/d5ra03971a

rsc.li/rsc-advances

[a]*Department of Clinical Laboratory Sciences, Faculty of Applied Medical Sciences, Umm Al-Qura University, Makkah, Kingdom of Saudi Arabia. E-mail: mmghaith@uqu.edu.sa*

[b]*Department of Biochemistry, Faculty of Medicine, Umm Al-Qura University, Al Abdeyah, Makkah, 24381, Saudi Arabia. E-mail: Ramaimani@uqu.edu.sa*

[c]*Botany and Microbiology Department, Faculty of Science, Suez Canal University, Ismailia, 41522, Egypt. E-mail: aghareeb@science.suez.edu.eg*

[d]*Medical Laboratory Technology Department, Faculty of Nursing and Health Sciences, Jazan University, Jazan, Saudi Arabia. E-mail: Mhabibullah@jazanu.edu.sa*

[e]*Department of Basic Medical Sciences, College of Medicine, AlMaarefa University, Diriyah, 13713, Riyadh, Saudi Arabia. E-mail: sfadl@um.edu.sa*

[f]*Department of Biological Sciences, Faculty of Science, University of Jeddah, Jeddah, Saudi Arabia. E-mail: haalomari@uj.edu.sa*

[g]*Biology Department, Faculty of Science, Islamic University of Madinah, Madinah, 42351, Saudi Arabia. E-mail: falbaqami@iu.edu.sa*

[h]*Department of Biology, Faculty of Science, Al-Baha University, Alaqiq, 65779-7738, Saudi Arabia. E-mail: falbeladi@bu.edu.sa*

[i]*Department of Medical Microbiology, Faculty of Medicine, University of Jeddah, 23218, Jeddah, Saudi Arabia. E-mail: anomani@uj.edu.sa*

[j]*Department of Pharmaceutical Sciences, College of Pharmacy, Princess Nourah Bint Abdulrahman University, P.O. Box 84428, Riyadh, 11671, Saudi Arabia. E-mail: aaalrashidi@pnu.edu.sa; szalshawwa@pnu.edu.sa*

[k]*Zoology Department, Faculty of Science, Ain Shams University, Cairo, 11566, Egypt. E-mail: Hanaafathy@sci.asu.edu.eg*

[l]*Research Center, Deanship of Scientific Research and Post-Graduate Studies, AlMaarefa University, Diriyah, 13713, Riyadh, Saudi Arabia*

1. Introduction

Over the last fifty years, studies have introduced numerous natural products purified from marine microorganisms with potential for the management of various diseases.[1] Bio-mining of unexplored marine microorganisms, which produce bioactive substances with numerous applications, holds great promise owing to their exclusive biomedical properties.[2] Marine microorganisms have adapted to extreme environments, including high pressure, temperature fluctuations, hypersalinity, and nutrient limitation, resulting in the evolution of rare and unique genetic traits and diverse mechanisms of action. This genetic and metabolic versatility often underpins the biosynthesis of distinctive secondary metabolites with a wide range of biological activities.[3–5] Around 28 500 marine natural products have been identified, comprising sterol-like products, peptides, polyphenolics, fatty acid-derivatives, terpenoids, alkaloids, polysaccharides, and other metabolites.[6] Microbial exopolysaccharides (EPS) are secondary metabolites that form a protective scaffold around cells. The EPS exhibit diverse physicochemical properties that support survival in extreme environments, such as deep-sea hydrothermal vents. Their primary roles include protection against heavy metal toxicity, dehydration, and environmental stress, while also promoting cell aggregation, surface adhesion, biofilm formation, and micronutrient uptake (Netrusov *et al.*, 2023, Vu *et al.*, 2009).[7] Currently, there is a significant focus on isolating and identifying new marine extremophilic bacteria capable of producing novel EPS. Various genera of marine bacteria, including *Alteromonas*, *Bacillus*, *Cobetia*, *Colwellia*, *Geobacillus*, *Halomonas*, *Hyphomonas*, *Idiomarina*, *Pseudoalteromonas*, *Polaribacter*, *Pseudomonas*, *Polaribacter*, *Rhodococcus*, *Shewanella*, and *Exiguobacterium*, *Planococcus* have been recognized as EPS producers.[8–11]

Microbial EPS display significant structural diversity, particularly in monosaccharide composition, which may include neutral sugars (*e.g.*, D-glucose, D-mannose, D-galactose, D-xylose, L-arabinose), deoxy sugars (*e.g.*, L-fucose), hexosamines (*e.g.*, D-glucosamine), and uronic acids (*e.g.*, D-galacturonic acid). Variability in glycosidic linkages (α- or β-configurations) and branching contributes to their complex architecture. The presence of anionic substituents and uronic acid residues imparts a net negative charge, influencing both physical and biological functions. This structural complexity confers advantageous properties such as high adhesiveness, gelation, viscoelasticity, pseudoplasticity, thixotropy, biocompatibility, biodegradability, and stability under extreme pH, temperature, and salinity conditions (Yildiz & Karatas, 2018; X. Sun & Zhang, 2021; J. Wang *et al.*, 2023).[12–14] Consequently, EPSs have broad industrial applications across the food, pharmaceutical, cosmetic, chemical, gas, and textile sectors. They function as thickeners (*e.g.*, binding agents, gelling agents), emulsifiers (*e.g.*, surfactants, dispersants), stabilizers, and coagulants (*e.g.*, polyacrylamide), contributing to product consistency and quality. Additionally, several marine-derived EPSs exhibit pharmacological properties, including notable antiviral activity against a range of viral pathogens.[15] Purified EPS derived from thermophilic *Bacillus licheniformis* demonstrated potent, dose-dependent antiviral activity against HSV-2 in human peripheral blood mononuclear cells. This effect was attributed to immunomodulatory mechanisms, as EPS treatment enhanced the expression of key cytokines involved in antiviral defense, including IFN-α, IFN-γ, TNF-α, IL-12, and IL-18.[16] Additionally, marine-derived EPSs have shown wound healing and anti-inflammatory properties, promoting tissue regeneration and accelerating all phases of the wound healing process.[17]

A growing interest has recently been directed to discover novel antimicrobial agents derived from marine bacteria aimed at addressing the threat posed by multidrug-resistant pathogens, which are increasingly challenging public health.[18] Several studies have reported antibacterial properties of EPS, particularly through the suppression of biofilm formation. For instance, Almutairi *et al.* observed that EPS derived from *Enterobacter* sp. ACD2, a bacterial species isolated from Tabuk, Saudi Arabia, demonstrated robust antimicrobial properties toward *Staphylococcus aureus* and *E. coli*.[19] The EPS molecular weight is a significant determinant that affects antibacterial activity. For example. mutant strain of *B. animalis* subsp. *lactis* producing high molecular weight EPS showed decreased attachment to human intestinal epithelial cells and a reduced capacity for biofilm formation.[20] Further, Rubini *et al.* stated that the chitosan from a marine polysaccharide source displays substantial antimicrobial properties and potent inhibition toward infectious uropathogenic *Escherichia coli* by disrupting quorum-sensing biofilm development.[21] Similarly, Wu *et al.* reported that the exopolysaccharide EPS273 from the marine *P. stutzeri* 273 inhibits *Pseudomonas aeruginosa* biofilm formation and disperses biofilm aggregation. EPS273 reduced the production of crucial virulence elements, attenuated the bacterium's virulence against human pulmonary cells, and decreased the levels of hydrogen peroxide and extracellular DNA.[22] Recently, we reported a novel EPS (EPSR5) derived from marine sediments in the Red Sea, specifically from the marine bacterium *Kocuria* sp. strain AG5 (Accession no. ON077051), and uncovered its potential and promising properties.[23] In the current study, we aimed to extend our investigations to further explore the structural characteristics of EPSR5 and its multi-target potential by evaluating its antimicrobial, antidiabetic, and wound healing potential.

2. Materials and methods

2.1. Samples and reagents

The EPSR5 sample was prepared as previously described by our group.[23] Unless otherwise specified, all chemical reagents and standards were purchased from Sigma-Aldrich, TCI, or Acros.

2.2. Structural characterization of EPSR5

2.2.1. Gas chromatography–mass spectrometry (GC–MS) analysis. EPSR5 was hydrolyzed and chemically derivatized prior to GC–MS analysis in order to convert its monosaccharide constituents into volatile silylated derivatives suitable for

separation. Briefly, the dried polysaccharide sample was subjected to acid hydrolysis, followed by drying under vacuum. The residue was then derivatized using *N*,*O*-bis(trimethylsilyl)trifluoroacetamide (BSTFA) containing 1% trimethylchlorosilane (TMCS) (Sigma-Aldrich, USA). The reaction mixture was incubated at 65 °C for 1 hour to ensure complete silylation, while minimizing moisture exposure to avoid degradation of the derivatives. The derivatized samples were analyzed on a Trace GC Ultra system coupled with a TSQ mass spectrometer (Thermo Scientific, Austin, TX, USA) equipped with a TG-5MS capillary column (30 m × 0.25 mm i.d., 0.25 μm film thickness). The oven program was initiated at 50 °C, ramped at 5 °C min^{-1} to 250 °C and held for 2 minutes, then increased at 30 °C min^{-1} to 300 °C and held for 2 minutes. The injector and transfer line temperatures were set at 270 °C and 260 °C, respectively. Helium (99.999% purity, Linde, Germany) was used as the carrier gas at a constant flow rate of 1 mL min^{-1}. A 1 μL aliquot of the derivatized sample was injected in split mode using an AS1300 autosampler (Thermo Scientific, USA), with a solvent delay of 2 minutes. The mass spectrometer was operated in electron ionization (EI) mode at 70 eV with the ion source at 200 °C. Spectra were acquired in full scan mode over the *m*/*z* range of 50–650. Individual compounds were identified by comparing their fragmentation patterns with reference spectra from the NIST 14 and WILEY 09 mass spectral libraries.[24]

2.2.2. HPLC analysis of EPSR5 monosaccharide composition. EPSR5 was first hydrolyzed to release its monosaccharide components. Briefly, 2 mL of trifluoroacetic acid (TFA, Sigma-Aldrich, USA) was added to the dried EPSR5 sample in a sealed vial under an argon atmosphere and incubated at 110 °C for 6 h. Following hydrolysis, the reaction mixture was evaporated under reduced pressure. To completely remove residual acid, methanol was added to the residue, and the drying step was repeated five times until the methanol had fully evaporated. The resulting hydrolysate was then dissolved in ultrapure water to a final volume of 10 mL. For derivatization, 0.3 M 1-phenyl-3-methyl-5-pyrazolone (PMP, Sigma-Aldrich, USA) in methanol, 0.2 M NaOH, and the hydrolysate were combined and incubated at 70 °C in a water bath for 1.5 h. The reaction was neutralized with 0.2 M HCl solution. The mixture was extracted with chloroform to remove excess PMP, then centrifuged at 4000 rpm for 10 min (Nuve, Turkey). The aqueous phase was filtered through a 0.22 μm PES membrane (Sartorius Stedim Biotech, Germany), and the filtrate was diluted 10-fold prior to injection. HPLC analysis was performed using a Thermo Ultimate 3000 system (Thermo Scientific, Italy) equipped with a UV detector set at 190 nm and a COL-Ca column (300 × 7.7 mm, Thermo Scientific, Italy). The separation was carried out under isocratic elution with ultrapure water as the mobile phase at a flow rate of 0.5 mL min^{-1} and a column temperature of 80 °C.

2.2.3. Thermal gravimetric analysis (TGA). The thermal stability and decomposition behavior of EPSR5 were assessed using a Simultaneous Thermogravimetric Analyzer (NEXTA STA200, Hitachi High-Tech Global, Japan). A weighed sample of EPSR5 (16.559 mg) was placed in a sealed aluminum pan and heated from 20 °C to 300 °C at a constant rate of 10 °C min^{-1} under a continuous flow of dry nitrogen gas at 20 mL min^{-1}. Indium was used as a calibration reference to ensure accurate temperature measurements. The resulting thermograms were analyzed to determine the thermal degradation profile and stability of EPSR5.[25,26]

2.2.4. Energy-dispersive X-ray (EDX) spectrometry. The elemental composition of EPSR5 was determined using energy-dispersive X-ray (EDX) spectroscopy, conducted on a JSM-7000 NeoScope™ benchtop scanning electron microscope (JEOL Ltd, Japan). The sample was analyzed based on characteristic emission peaks corresponding to specific elements in the electromagnetic spectrum. The elemental profile was obtained by detecting and quantifying the intensity of these peaks, allowing identification of the major elements present in the EPSR5 structure.

2.2.5. Scanning electron microscopy. The surface morphology of EPSR5 was examined using a JCM-7000 NeoScope™ benchtop scanning electron microscope (JEOL Ltd, Japan) operated at an accelerating voltage of 15 kV. The sample was mounted onto a specimen stub and coated with a thin layer of platinum to enhance conductivity and image quality. High-resolution SEM images were captured to assess the microstructural features and surface texture of EPSR5.[27]

2.3. Pathogen species

A total of seven pathogenic microbial strains were used in this study (VACSERA, Holding Company for Biological Products and Vaccines, SAE, Cairo, Egypt), including two Gram-positive bacteria, three Gram-negative bacteria, and two fungal species. The fungal strains were *Mucor circinelloides* (AUMMC 11656) and *Candida albicans* (ATCC 10221). The Gram-positive bacteria included *Enterococcus faecalis* (ATCC 10541) and *Staphylococcus aureus* (ATCC 6538). The Gram-negative bacterial strains comprised *Escherichia coli* (ATCC 8739), *Salmonella typhi* (ATCC 6539), and *Helicobacter pylori* (NCTC 11637).

2.4. Antimicrobial assessment

The antimicrobial activity of EPSR5 was evaluated using the agar well diffusion method, following the guidelines of the National Committee for Clinical Laboratory Standards (NCCLS, 2002). Bacterial strains were cultured in Nutrient Broth (Merck, Germany) and incubated at 37 °C for 18–24 hours. The turbidity was adjusted to the 0.5 McFarland standard, corresponding to approximately 1.5×10^8 CFU mL^{-1}. Fungal strains were grown in Sabouraud Dextrose Broth (Merck, Germany) at 25–30 °C for 48–72 hours and similarly standardized to 0.5 McFarland (approx. 1–5 × 10^6 CFU mL^{-1}). Mueller–Hinton Agar (Thermo Fisher Scientific, USA) plates were uniformly inoculated with 100 μL of the prepared bacterial or fungal suspensions. Wells of approximately 6–8 mm in diameter were created using a 25-gauge syringe and filled with 100 μL of the EPSR5 extract. Gentamicin sulfate (10 mg mL^{-1}, Sigma-Aldrich, Germany) was used as the positive control for bacterial strains, and fluconazole (10 mg mL^{-1}, Sigma-Aldrich, Germany) served as the reference antifungal agent. Dimethyl sulfoxide (DMSO, Sigma-Aldrich, Germany) was used as the negative control. The

plates were incubated at 37 °C for 18–24 hours for bacterial cultures and at 25–30 °C for 24–48 hours for fungal cultures. Antimicrobial activity was determined by measuring the diameter of the inhibition zones in millimeters.[28,29]

2.5. Minimal inhibitory concentration (MIC) assessment

The minimal inhibitory concentration (MIC) of EPSR5 against the tested microbial strains was determined using the broth microdilution method. Briefly, 0.1 mL of sterile Mueller–Hinton Broth (Merck, Germany) was dispensed into each well of a sterile 96-well microtiter plate (Nunc, Thermo Fisher Scientific, USA). Serial twofold dilutions of EPSR5 were prepared in broth, starting from a stock solution of 1000 μg mL^{-1}, obtained by dissolving 10 mg of EPSR5 in 10 mL of distilled water (Milli-Q grade). The final concentrations tested ranged from 1000 to 7.8 μg mL^{-1}. Microbial inocula were prepared by suspending freshly grown colonies in 0.85% saline (Merck, Germany) or broth, adjusting turbidity to the 0.5 McFarland standard (approx. 1.5×10^8 CFU mL^{-1} for bacteria), and diluting to achieve a final inoculum of approximately 5×10^5 CFU per mL per well. Within 15 minutes of preparation, 100 μL of the standardized microbial suspension was added to each well containing EPSR5 dilutions. Control wells included broth only (sterility control) and broth with inoculum but without EPSR5 (growth control). The plates were then sealed and incubated at 35 ± 2 °C for 16–20 hours. MIC was defined as the lowest concentration of EPSR5 that visibly inhibited microbial growth, as indicated by the absence of turbidity. Results were reported in micrograms per milliliter (μg mL^{-1}).[30]

2.6. Minimum bactericidal concentration (MBC) and minimum fungal concentration (MFC) assessment

To determine the minimum bactericidal concentration (MBC) of EPSR5, 100 μL aliquots were taken from MIC-negative wells (showing complete inhibition of visible growth) and from the corresponding positive growth controls. These samples were subcultured onto Mueller–Hinton agar plates and incubated at 35 °C for 72 hours. The MBC was defined as the lowest concentration of EPSR5 that prevented the appearance of bacterial colonies, indicating complete microbial killing rather than mere growth inhibition. The MBC/MIC ratio was used to assess the nature of the antibacterial effect, with a ratio ≤4 considered indicative of bactericidal activity. All experiments were performed in triplicate to ensure reproducibility.[31] For evaluation of the minimum fungicidal concentration (MFC), the method described by Espinel-Ingroff (2001) was followed. After 72 hours of incubation, 20 μL was taken from wells showing no visible fungal growth, including the MIC-negative and adjacent positive growth control wells. Each sample was subcultured onto Sabouraud dextrose agar (Merck, Germany) plates and incubated at 35 °C for 48 hours. The MFC was defined as the lowest concentration of EPSR5 that resulted in three or fewer colonies, corresponding to a fungicidal effect of approximately 99–99.5% cell death. Similar to the MBC criterion, EPSR5 was considered fungicidal when the MFC/MIC ratio was ≤4.[32]

2.7. Anti-biofilm activity

The anti-biofilm potential of EPSR5 was assessed using a 96-well flat-bottom polystyrene microtiter plate assay (Nunc, Thermo Fisher Scientific, USA), based on the method described by Antunes *et al.*, with minor modifications.[33] Test organisms were cultured in trypticase soy yeast (TSY) broth (Sigma-Aldrich, Germany) and adjusted to a final concentration of 10^6 CFU mL^{-1}. Each well was filled with 300 μL of the inoculated broth, and EPSR5 was added at sublethal concentrations corresponding to 75%, 50%, and 25% of the previously determined MBC. Control wells included uninoculated medium (blank) and inoculated medium without EPSR5 (negative control). Plates were incubated at 37 °C for 48 hours to allow biofilm formation. After incubation, the supernatant was carefully discarded, and wells were washed thoroughly with sterile distilled water to remove non-adherent cells. To fix and stain the remaining biofilm, each well was treated with 250 μL of 95% ethanol (Merck, Germany) to dissolve the crystal violet stain (0.1% w/v, Sigma-Aldrich, Germany). After a 15 minute incubation, the absorbance was measured at 570 nm using a microplate reader (BioTek, USA). The percentage of biofilm inhibition by EPSR5 was calculated using the following formula:

$$\text{Biofilm inhibition ability} = \left(1 - \frac{\text{absorbance of sample} - \text{absorbance of blank}}{\text{absorbance of conrol} - \text{absorbance of blank}}\right) \times 100$$

where the blank represents the absorbance of the medium alone, the sample indicates the absorbance of the test organism treated with EPSR5, and the control shows the absorbance of the untreated test organism. This procedure was performed in triplicate.

2.8. α-Amylase inhibitory activity

The α-amylase inhibitory activity of EPSR5 was assessed using the 3,5-dinitrosalicylic acid (DNSA) method as described by Wickramaratne *et al.*, with slight modifications.[34] This assay was conducted to evaluate the potential of EPSR5 in regulating pancreatic enzyme activity and glycemic control. EPSR5 was initially dissolved in a small volume of 10% DMSO and then diluted with phosphate buffer (0.02 M Na_2HPO_4/NaH_2PO_4, 0.006 M NaCl, pH 6.9, Merck, Germany) to yield final concentrations ranging from 1.9 to 1000 μg mL^{-1}. In each reaction mixture, 200 μL of α-amylase solution (2 units per mL, Sigma-Aldrich, USA, EC 3.2.1.1) was mixed with 200 μL of EPSR5 solution and incubated at 30 °C for 10 minutes. Subsequently, 200 μL of a 1% (w/v) starch solution was added to each tube, followed by a 3 minute incubation period to initiate the enzymatic reaction. The reaction was terminated by adding 200 μL of DNSA reagent, which consisted of 12 g of sodium potassium tartrate tetrahydrate (Rochelle salt) dissolved in 8 mL of 2 M NaOH and 20 mL of 96 mM DNSA solution (all from Sigma-Aldrich, USA). The reaction mixtures were then heated at 85–90 °C for 10 minutes, cooled to room temperature, and diluted with 5 mL of distilled water. The absorbance was measured at 540 nm using a UV-Visible spectrophotometer (Biosystem 310). A control sample (representing 100% enzyme activity) was

prepared by replacing EPSR5 with phosphate buffer. A reagent blank was also included by omitting the enzyme from the reaction. The percentage inhibition of α-amylase activity was calculated using the following formula:

$$\%\ \alpha\text{-amylase inhibition} = 100 \times \frac{\text{absorbance of control} - \text{absorbance of sample}}{\text{absorbance of control}}$$

The percent α-amylase inhibition was plotted against the concentration of EPSR5. IC_{50} values, which denote the concentration of EPSR5 necessary to inhibit 50% of α-amylase activity, were determined from these plots.

2.9. α-Glucosidase inhibitory activity

The α-glucosidase inhibitory activity of EPSR5 was evaluated using the method described by Pistia-Brueggeman and Hollingsworth, with slight modifications.[35] This assay is critical for assessing antidiabetic potential, as α-glucosidase inhibitors delay carbohydrate digestion and glucose absorption, thereby reducing postprandial blood glucose levels. EPSR5 was tested at concentrations ranging from 1.97 to 1000 μg mL^{-1}. In a typical assay, 50 μL of the EPSR5 solution was added to 10 μL of α-glucosidase enzyme solution (1 U mL^{-1}, Sigma-Aldrich, USA), followed by 125 μL of 0.1 M phosphate buffer (pH 6.8; Merck, Germany). The mixture was incubated at 37 °C for 20 minutes. After incubation, 20 μL of 1 M *p*-nitrophenyl-α-D-glucopyranoside (*p*NPG, Sigma-Aldrich, USA) was added as the substrate to initiate the enzymatic reaction. The reaction was allowed to proceed for 30 minutes and was then terminated by adding 50 μL of 0.1 N Na_2CO_3. Absorbance was measured at 405 nm using a Biosystem 310 Plus spectrophotometer. The percentage inhibition of α-glucosidase activity was calculated using the following formula:

$$\text{Glucosidase inhibition}\% = 100 - \frac{\text{OD blank} - \text{OD sample}}{\text{OD blank}} \times 100$$

where OD blank refers to the absorbance of the enzyme in the absence of samples, and OD sample indicates the absorbance of the enzyme in the presence of the sample. The IC_{50} value was calculated using the regression equation obtained by plotting concentrations between 1.95 and 1000 μg mL^{-1} against the percentage inhibition for EPSR5.[36]

2.10. Antioxidant activity

2.10.1. Total antioxidant capacity (TAC) by phosphomolybdenum assay. The total antioxidant capacity of EPSR5 was evaluated using the phosphomolybdenum assay, as described by Prieto *et al.*, with minor modifications.[37] This method is based on the reduction of molybdenum (Mo^{6+}) to molybdenum (Mo^{5+}) by antioxidant compounds, resulting in the formation of a green phosphate/Mo^{5+} complex in an acidic environment. To perform the assay, 1 mL of EPSR5 solution (0.5 mg mL^{-1}) was mixed with 3 mL of reagent solution containing 0.6 M sulfuric acid (H_2SO_4), 28 mM sodium phosphate (NaH_2PO_4), and 4 mM ammonium molybdate. A blank control was prepared using 4 mL of the reagent solution without EPSR5. The reaction mixtures were incubated at 95 °C for 150 minutes in a water bath. After cooling to room temperature, the absorbance was measured at 630 nm using a microplate reader (Biotek ELX800, Biotek Instruments, Winooski, VT, USA). The antioxidant activity was expressed as ascorbic acid equivalents (AAE) in μg mg^{-1} of EPSR5, based on a standard calibration curve constructed with known concentrations of ascorbic acid.[38]

2.10.2. Ferric reducing antioxidant power (FRAP) assay. The ferric reducing antioxidant power (FRAP) of EPSR5 was evaluated using the potassium ferricyanide–trichloroacetic acid method, adapted from Benzie and Strain[39] and modified for microplate application as described by Athamena *et al.*[40] This assay measures the ability of EPSR5 to reduce ferric (Fe^{3+}) to ferrous (Fe^{2+}) ions, forming a blue-colored Fe^{2+}-TPTZ complex under acidic conditions, with absorbance measured at 630 nm. For each reaction, 40 μL of EPSR5 solution was mixed with 50 μL of 1% potassium ferricyanide [$K_3Fe(CN)_6$], 50 μL of 10% trichloroacetic acid (TCA), and 50 μL of 0.2 mol L^{-1} sodium phosphate dihydrate ($Na_2HPO_4 \cdot 2H_2O$) buffer in labeled Eppendorf tubes. The mixtures were incubated and then centrifuged at 3000 rpm for 10 minutes. Following centrifugation, 166.66 μL of the clear supernatant was transferred into a 96-well microtiter plate, followed by the addition of 33.3 μL of 1% ferric chloride ($FeCl_3$). DMSO served as the negative control, while ascorbic acid (1 mg mL^{-1}) was used as the positive reference standard. The absorbance was recorded at 630 nm using a microplate reader (Biotek ELX800, Biotek Instruments, Winooski, VT, USA). The results were expressed as ascorbic acid equivalents (AAE) in mg mg^{-1} of EPSR5.

2.11. Pancreatic lipase inhibition assay

The pancreatic lipase inhibitory activity of EPSR5 was evaluated using *p*-nitrophenyl butyrate (pNPB, Sigma-Aldrich, USA) as a substrate, following a modified version of the method described by Kim *et al.*[41] The assay was designed to assess the ability of EPSR5 to interfere with triglyceride digestion by comparing lipase activity in the presence and absence of the test compound. The substrate solution was prepared by dissolving PNPB at a concentration of 1 mg mL^{-1} in 0.1 mM potassium phosphate buffer (pH 6.0) containing acetonitrile, and the final volume was adjusted to 10 mL. The solution was stored at −20 °C until use. The lipase enzyme (porcine pancreatic lipase, Spectrum Diagnostics, Egypt) was freshly prepared before the assay by dissolving 10 mg of the enzyme in 10 mL of phosphate buffer (1 mg mL^{-1}) with gentle mixing. EPSR5 and Orlistat (positive control, Sigma-Aldrich, USA) were tested at concentrations ranging from 7.8 to 1000 μg mL^{-1}. Each sample or control was preincubated with lipase for 1 hour in 0.1 mM potassium phosphate buffer (pH 7.2) containing 0.1% Tween 80 (Merck, Germany) at 30 °C. The reaction was initiated by adding 0.1 μL of the PNPB substrate to achieve a final reaction volume of 100 μL. After a 5 minute incubation at 30 °C, the release of *p*-nitrophenol was measured spectrophotometrically at 405 nm using a Biosystem 310 Plus UV-Visible spectrometer. DMSO was

used as the negative control. The lipase inhibitory activity was calculated using the following formula.

$$\text{Inhibitory activity } (I\%) = 100 - \frac{(B-b)}{(A-a)} \times 100$$

where A is the absorbance of lipase activity without inhibitor, a is the absorbance of the negative control (DMSO) without inhibitor and lipase, B is the absorbance of lipase activity with inhibitor, and b is the absorbance of the negative control (sample in DMSO) with inhibitor and without lipase.

2.12. Wound healing activity

The scratch assay was performed as described by Rötzer *et al.*, with slight modifications.[42] Confluent monolayers of cultured cells were mechanically scratched using a sterile pipette tip to create a wound gap. The cells were then treated with EPSR5 and incubated under standard conditions. Two primary parameters were used to assess the wound healing response: wound width and wound area. Wound width was calculated by measuring the average distance between the edges of the scratch at defined time intervals. The cell migration rate was determined by calculating the reduction in wound width over time. In addition, the wound area was quantified using ImageJ software (NIH, Bethesda, MD) by measuring the cell-free area within the scratch zone. A progressive decrease in wound area over time indicated effective cell migration and healing. The percentage of wound closure was computed to reflect the healing efficiency and was expected to increase proportionally with cell migration. These results provided quantitative insights into the pro-migratory and wound-reparative effects of EPSR5 on epithelial cells.

3. Results

3.1. Structural characterization profile of EPSR5

In our previous study, we reported essential chemical composition data of EPSR5, including sulfate (25.6%), uronic acid (21.77%), and total hexosamine (13.55%) contents. The polymer was further shown to have an average molecular weight of 4.9×10^4 g mol^{-1} and a polydispersity index of 1.1, with FTIR spectra confirming polysaccharide functional groups (O–H, C=O, SO_3^-, and β-pyranose signals). These results established EPSR5 as a high-molecular weight, acidic heteropolysaccharide.[23] To complement our previously reported chemical and spectroscopic data, we further applied advanced characterization techniques to explore its detailed monosaccharide composition, the surface morphology and elemental composition, and the thermal stability and degradation behavior. In this regard, we have performed a set of analytical techniques, including GC-MS analysis, thermogravimetric analysis, and SEM-EDX analysis.

3.1.1. Analysis of EPSR5 monosaccharide composition by GC–MS and HPLC. To gain insight into the monosaccharide constituents of EPSR5, the polymer was hydrolyzed, derivatized with BSTFA + 1% TMCS to generate volatile trimethylsilyl derivatives, and analyzed by GC–MS. The resulting chromatogram displayed several well-resolved peaks corresponding to silylated derivatives of neutral and acidic sugars (Fig. 1). Two distinct peaks were assigned to arabinose derivatives, reflecting the known tendency of monosaccharides to yield multiple silylated forms depending on their anomeric configuration and ring structure. A peak at RT 20.49 min was identified as methyl α-arabinofuranoside (3TMS derivative), while a second peak at RT 21.10 min corresponded to arabinose (4TMS derivative). A distinct peak at RT 25.89 min was identified as D-(+)-xylose (4TMS derivative). A major peak was observed at RT 27.17 min, which was assigned to D-glucose (5TMS derivative), confirming that glucose represents a dominant monosaccharide in EPSR5. In addition, a significant peak detected at RT 28.86 min was identified as glucuronic acid (5TBDMS derivative), indicative of the incorporation of uronic acid residues within the polymer backbone. The identification of these four monosaccharides demonstrates that EPSR5 is a heteropolysaccharide composed of both neutral and acidic sugars. Notably, the presence of glucuronic acid corroborates the relatively high uronic acid content (21.77%) previously determined by chemical analysis,[23] thereby reinforcing the polyanionic character of this polymer. To further validate the GC–MS results and quantify the relative monosaccharide composition of EPSR5, the hydrolyzed sample was derivatized with PMP and analyzed by HPLC. The chromatogram revealed four distinct peaks corresponding to arabinose, glucose, glucuronic acid, and xylose (Fig. 1). The retention times and relative peak areas indicated that glucose was the predominant monosaccharide (RT 9.06 min, 59.64%), followed by xylose (RT 15.95 min, 28.49%), glucuronic acid (RT 12.89 min, 7.37%), and arabinose (RT 5.25 min, 4.51%). These quantitative data demonstrate that EPSR5 is a glucose-rich heteropolysaccharide, with xylose contributing substantially, while arabinose and glucuronic acid are present in smaller proportions. The detection of glucuronic acid supports the significant uronic acid content (21.77%) previously determined by chemical assays, confirming the polyanionic character of the polymer. Together, the complementary GC–MS and HPLC analyses conclusively established that EPSR5 is a heteropolysaccharide composed primarily of glucose and xylose, with smaller amounts of arabinose and glucuronic acid. The detection and quantification of glucuronic acid further support its high uronic acid content, confirming the polyanionic and acidic nature of the polymer.

3.1.2. Thermogravimetric analysis (TGA). To examine the thermal stability and degradation profile of EPSR5, we performed thermogravimetric analysis (TGA). The TGA profile of EPSR5 revealed four distinct thermal degradation stages (Fig. 1). The first stage, observed at ambient temperatures up to 74.6 °C, showed a slight weight loss of approximately 258.8 mg. This initial loss is attributed to the evaporation of physically adsorbed water molecules, particularly those associated with carboxyl groups in the polymer structure. The second stage, beginning at 139.8 °C, exhibited a further weight loss of 54.0 mg. This phase likely corresponds to the decomposition of thermally labile functional groups present in the EPS, indicating the onset of structural instability. The third stage occurred over a broad temperature range, from 257.07 °C to

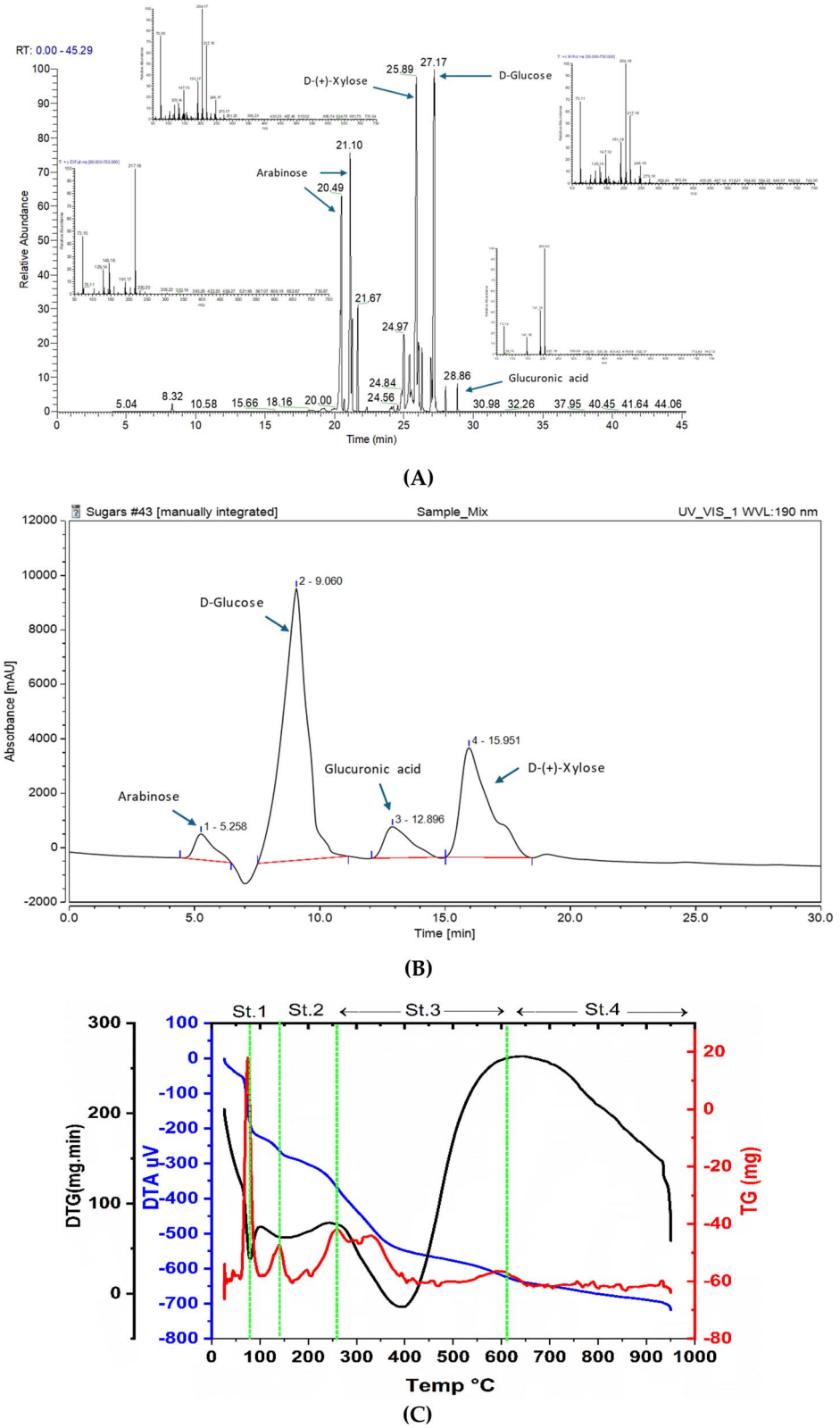

Fig. 1 Characteristic spectral analysis of EPSR5 extract produced by *Kocuria* sp. strain AG5. (A and B) GC-MS and HPLC analysis of EPSR5 extract showing the monosaccharide composition. (C) TGA-DTG graphical analysis of EPSR5 extract showing the thermal stability and degradation behavior of EPSR5.

644.46 °C, with a recorded weight loss of 70.7 mg. This major decomposition phase is associated with the breakdown of C–C and C–O bonds within the pyranose rings, leading to depolymerization and the thermal degradation of the polysaccharide backbone. The release of gaseous products such as H_2O, CO, and CO_2 supports this interpretation. The final stage began at approximately 644.46 °C, where the formation of carbonaceous char was observed, accompanied by a final weight loss of 55.5 mg. Overall, these results indicate that the exopolysaccharide EPSR5 produced by *Kocuria* sp. strain AG5 is thermally stable up to 257.07 °C, making it a promising candidate for applications requiring moderate thermal resistance.

3.1.3. SEM-EDX analysis. The surface morphology and microstructure of EPSR5 were examined using Scanning Electron Microscopy (SEM), as shown in Fig. 2. The SEM images revealed that EPSR5 consists of irregularly shaped, porous flakes with a smooth and glossy surface texture, suggesting a non-crystalline, amorphous structure. Energy-dispersive X-ray spectroscopy (EDX) analysis further confirmed the elemental composition of EPSR5, indicating the presence of oxygen, sodium, and phosphorus. Quantitative EDX data showed a high proportion of oxygen (47.87%), followed by sodium (25.34%) and phosphorus (26.79%) (Fig. 2D). The high oxygen content is typical of polysaccharide structures, while the presence of phosphorus suggests possible phosphorylation of the polysaccharide chains. Phosphorylation can occur through the substitution of hydroxyl groups by phosphate groups, either naturally or during extraction or processing. Together, the SEM and EDX analyses revealed valuable insights into the physical structure and chemical composition of EPSR5, supporting its biomedical applicability.

3.2. Assessment of the anti-microbial effect

Antimicrobial activity refers to the ability of a compound to inhibit or destroy the growth and reproduction of microorganisms, including bacteria and fungi. Several plant-derived polysaccharides have been reported to exhibit notable antibacterial and antifungal properties. In the present study, the antimicrobial activity of EPSR5 was evaluated against a panel of antibiotic-sensitive and resistant microbial strains by measuring the diameter of growth inhibition zones (in mm) in an agar well diffusion assay (Fig. 3). Gentamicin was used as the standard control for antibacterial activity, while fluconazole served as the antifungal control. EPSR5 exhibited a considerable increase in the inhibition zone diameter, indicating strong antimicrobial potency in comparison to the reference drugs. EPSR5 demonstrated significant antibacterial activity against both Gram-positive and Gram-negative bacteria. Specifically, treatment with EPSR5 resulted in markedly larger inhibition zones against *Enterococcus faecalis*, *Helicobacter pylori*, *Escherichia coli*, and *Salmonella typhi* compared to gentamicin, suggesting superior efficacy. In contrast, no significant difference in inhibition was observed against *Staphylococcus aureus*

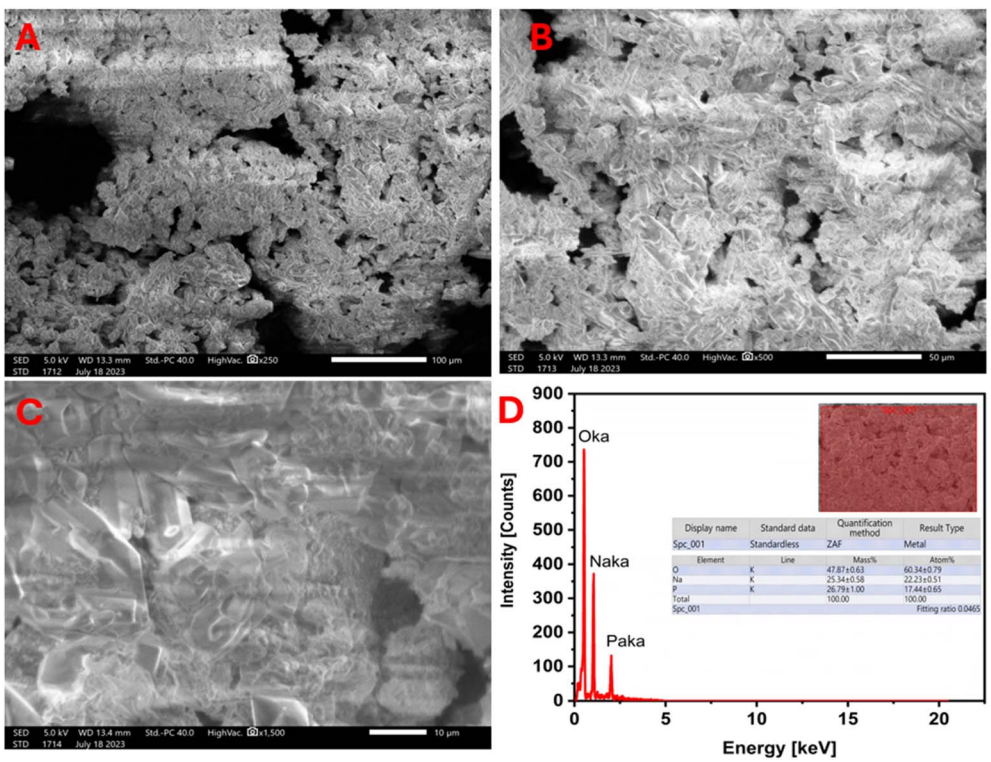

Fig. 2 SEM and EDX analysis of the EPSR5 polymer produced by *Kocuria* sp. strain AG5. (A) SEM image showing the overall surface morphology at ×250 magnification (scale bar: 100 nm); (B) higher magnification view at ×500 (scale bar: 50 nm); (C) detailed surface texture at ×1500 magnification (scale bar: 10 nm); (D) EDX spectrum showing the elemental composition of EPSR5.

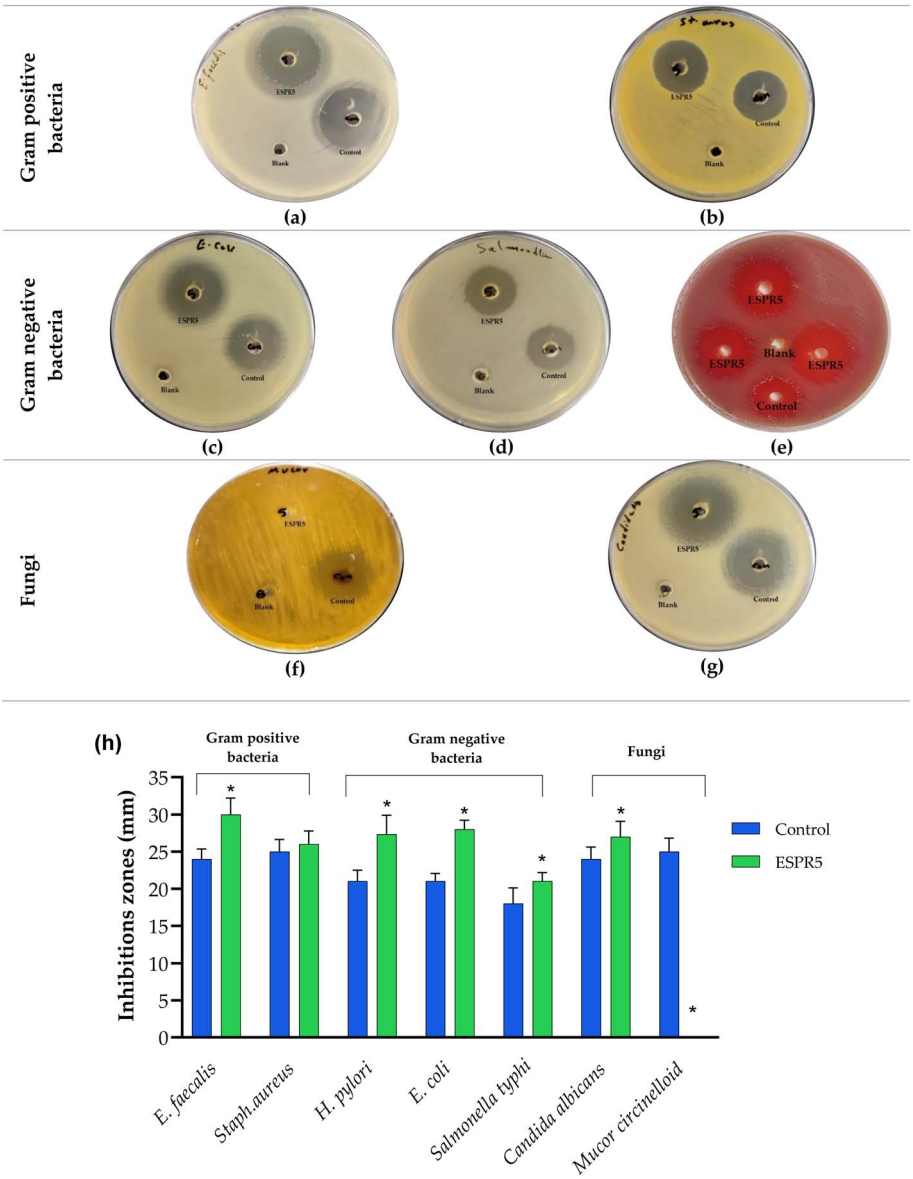

Fig. 3 Antimicrobial activity of EPSR5 against selected bacterial and fungal strains. (a) *Enterococcus faecalis* and (b) *Staphylococcus aureus* (Gram-positive bacteria); (c) *Escherichia coli*, (d) *Salmonella typhi*, and (e) *Helicobacter pylori* (Gram-negative bacteria); (f) *Mucor circinelloides* and (g) *Candida albicans* (fungi); (h) quantitative representation of inhibition zone diameters (mm) for all tested microorganisms following treatment with EPSR5. Data is presented as mean ± SD, with $n = 3$ experiments.

relative to the gentamicin control. In terms of antifungal activity, EPSR5 showed a pronounced inhibitory effect against *Candida albicans*, producing significantly larger inhibition zones than fluconazole. However, no antifungal activity was detected against *Mucor circinelloides*, as evidenced by the absence of inhibition zones, indicating resistance to EPSR5. These findings indicate that EPSR5 possesses broad-spectrum antimicrobial properties, with notable activity against several Gram-positive and Gram-negative bacteria as well as *Candida albicans*. The lack of effect against *Mucor circinelloides* highlights the selective nature of its antifungal action. This antimicrobial potential suggests possible applications of EPSR5 as a natural therapeutic.

3.3. Assessment of MIC, MFC, and MBC

To further evaluate the antimicrobial potential of EPSR5, its minimum inhibitory concentration (MIC), minimum bactericidal concentration (MBC), and minimum fungicidal concentration (MFC) were determined against selected bacterial and fungal strains (Fig. 4). For antifungal testing, MIC was assessed only for *Candida albicans*, as EPSR5 showed no inhibitory effect against *Mucor circinelloides*. The MIC value for *C. albicans* was 62.5 μg mL^{-1}, indicating that this low concentration was sufficient to inhibit fungal growth. Furthermore, the minimum fungicidal concentration (MFC) was established at 250 μg mL^{-1}, representing the lowest concentration required to completely eliminate *C. albicans* growth. These results suggest that EPSR5

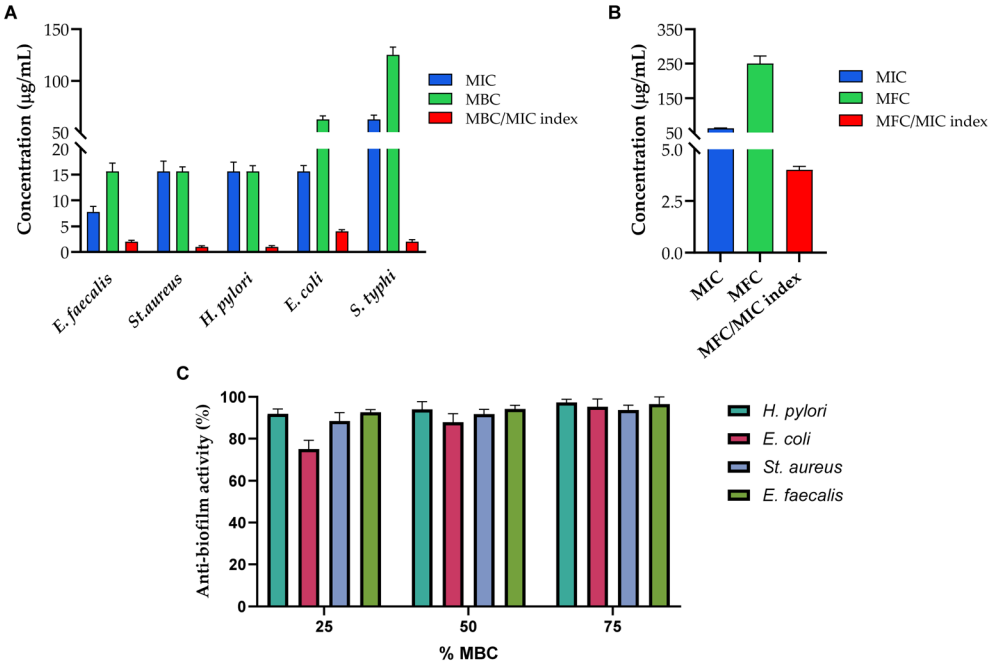

Fig. 4 The assessment of antimicrobial efficiency and antibiofilm activity of EPSR5 against selected bacterial and fungal strains. (a) MIC/MBC index for selected bacterial strains, (b) MIC/MFC for *Candida albicans* (c) percentage of antibiofilm activity of EPSR5 on different bacterial strains. Data is presented as mean ± SD, with $n = 3$ experiments.

has a promising antifungal effect against *C. albicans*, though further studies with additional fungal species are necessary to confirm its broader antifungal spectrum. In the antibacterial assessment, EPSR5 demonstrated potent activity against five clinically relevant bacterial strains. The MIC values were determined as follows: *Enterococcus faecalis* (7.8 µg mL^{-1}), *Staphylococcus aureus* (15.62 µg mL^{-1}), *Helicobacter pylori* (15.62 µg mL^{-1}), *Escherichia coli* (15.62 µg mL^{-1}), and *Salmonella typhi* (62.5 µg mL^{-1}). Notably, *E. faecalis* exhibited the highest sensitivity to EPSR5, requiring the lowest concentration for inhibition. Corresponding MBC values were found to be 15.62 µg mL^{-1} for *E. faecalis*, *S. aureus*, and *H. pylori*, 62.5 µg mL^{-1} for *E. coli*, and 125 µg mL^{-1} for *S. typhi*, confirming the effective antibacterial action of EPSR5. To distinguish between bactericidal and bacteriostatic effects, the MBC/MIC ratio was calculated. EPSR5 showed bactericidal activity against *S. aureus* and *H. pylori*, as the MIC and MBC values were identical. In contrast, a bacteriostatic effect was observed for *E. faecalis*, *E. coli*, and *S. typhi*, where MBC values were higher than the respective MICs. Overall, these results demonstrate that EPSR5 possesses broad-spectrum antimicrobial activity with both bacteriostatic and bactericidal properties depending on the target microorganism. Its low MIC and MFC/MBC values against clinically relevant pathogens, particularly *E. faecalis*, *S. aureus*, *H. pylori*, and *C. albicans*, indicate that EPSR5 is a promising candidate for development as a natural antimicrobial agent.

3.4. Assessment of anti-biofilm activity

Next, we envisioned the anti-biofilm activity of EPSR5 toward different bacterial strains. To evaluate the anti-biofilm activity of EPSR5, the extract was added to the culture media at the beginning of the incubation period. Following incubation, biofilms formed in microtiter wells were stained using crystal violet, and the absorbance was measured to quantify biofilm mass. The efficacy of EPSR5 in inhibiting biofilm formation was assessed by determining the percentage of biofilm reduction across different concentrations. In this study, *Helicobacter pylori* and *Escherichia coli* were used as representative Gram-negative bacteria, while *Enterococcus faecalis* and *Staphylococcus aureus* were chosen as representative Gram-positive bacteria (Fig. 4). At 75% of the minimum bactericidal concentration (MBC) of EPSR5, the biofilm inhibition percentages were remarkably high: 97.39% for *H. pylori*, 96.54% for *E. faecalis*, 95.25% for *E. coli*, and 93.71% for *S. aureus*. Similarly, at 50% of MBC, EPSR5 maintained strong anti-biofilm activity, with inhibition rates of 94.18% (*E. faecalis*), 94.03% (*H. pylori*), 91.78% (*S. aureus*), and 87.91% (*E. coli*). Even at 25% of MBC, notable inhibition was observed, with rates of 92.6% (*E. faecalis*), 91.89% (*H. pylori*), 88.49% (*S. aureus*), and 75.03% (*E. coli*). These findings demonstrate that EPSR5 possesses strong anti-biofilm properties against both Gram-positive and Gram-negative pathogens. The consistent reduction in biofilm formation across multiple concentrations suggests that EPSR5 effectively disrupts bacterial biofilm development pathways. Notably, the high level of inhibition even at sub-inhibitory concentrations indicates that EPSR5 could serve as a promising natural agent for biofilm control, with potential applications in combating biofilm-associated infections and enhancing antimicrobial therapies.

3.5. Assessment of antidiabetic activity

3.5.1. Assessment of α-amylase activity. Elevated α-amylase activity is associated with increased blood glucose levels and is

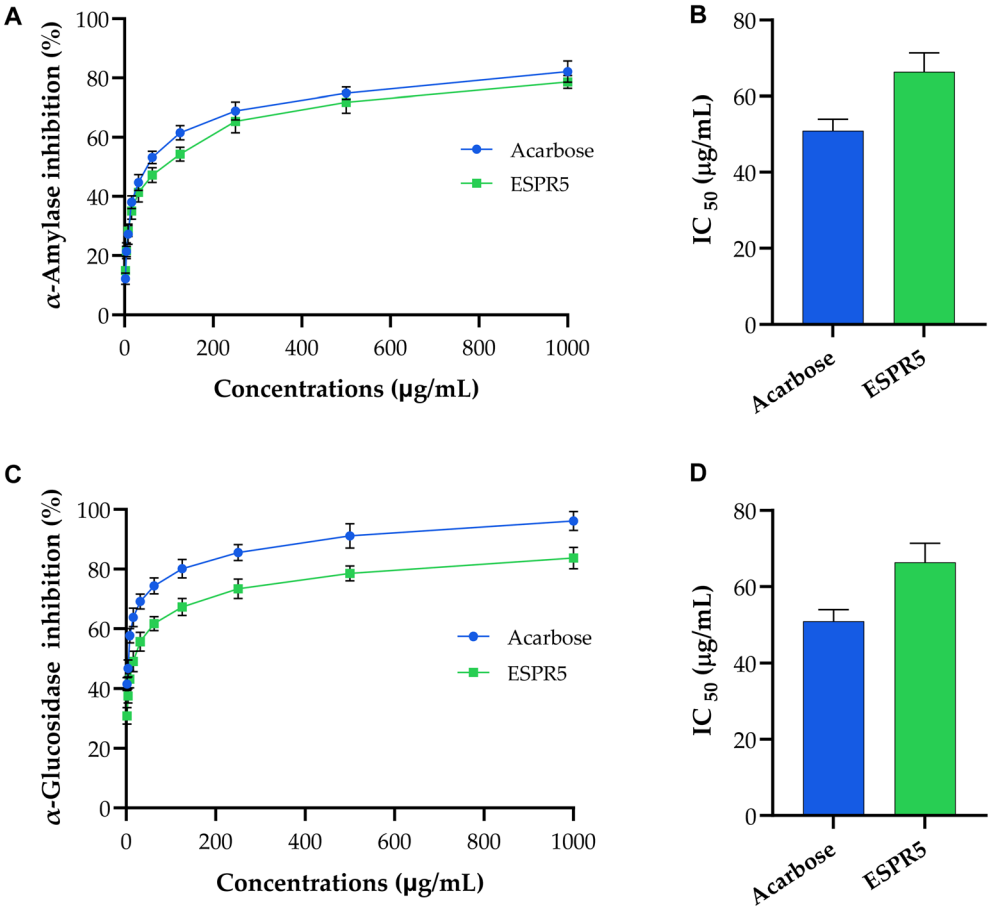

Fig. 5 The inhibitory activity of EPSR5 toward α-amylase and α-glucosidase enzymes. The dose-dependent inhibitory activity and IC_{50} value of EPSR5 as compared to acarbose toward α-amylase (A and B) and α-glucosidase (C and D). Data is presented as mean ± SD, with $n = 3$ experiments.

a contributing factor in the development of diabetes. To investigate the potential antidiabetic properties of EPSR5, we evaluated its inhibitory effect on α-amylase, a key enzyme involved in carbohydrate metabolism. α-Amylase hydrolyzes the α-1,4-glycosidic bonds in starch, converting it into oligosaccharides and glucose. In this study, various concentrations of EPSR5 (ranging from 1.95 to 1000 μg mL^{-1}) were tested for their ability to inhibit α-amylase activity. The percentage of enzyme inhibition was measured and compared to that of acarbose, a well-established antidiabetic drug known for inhibiting both α-amylase and α-glucosidase. As shown in Fig. 5, EPSR5 significantly inhibited α-amylase activity in a dose-dependent manner. The IC_{50} of EPSR5 was determined to be 66.35 μg mL^{-1}, which is slightly higher than that of acarbose (IC_{50} = 50.93 μg mL^{-1}), but still reflects a substantial inhibitory potential. These findings demonstrate that EPSR5 possesses noteworthy α-amylase inhibitory activity, suggesting that it may have antidiabetic potential through the modulation of carbohydrate digestion and postprandial glucose levels.

3.5.2. Assessment of α-glucosidase activity. α-Glucosidase is an essential enzyme secreted by the small intestine that hydrolyzes glucosidic bonds in carbohydrates, converting them into glucose units. Inhibiting this enzyme can effectively reduce postprandial hyperglycemia, making α-glucosidase inhibition a promising therapeutic strategy for managing type 2 diabetes. In this study, the potential of EPSR5 to inhibit α-glucosidase activity was evaluated across a range of concentrations (1.95 to 1000 μg mL^{-1}) and compared to acarbose, a well-known antidiabetic reference drug. As shown in Fig. 5, EPSR5 significantly inhibited α-glucosidase activity in a dose-dependent manner, with an IC_{50} value of 17.06 μg mL^{-1}. Although less potent than acarbose (IC_{50} = 4.13 μg mL^{-1}), EPSR5 still demonstrated a notable inhibitory effect, indicating its potential as a natural α-glucosidase inhibitor. Interestingly, EPSR5 was also shown to inhibit α-amylase activity, suggesting a dual mechanism of action. The simultaneous inhibition of both α-amylase and α-glucosidase represents a promising approach for controlling blood glucose levels and managing diabetes. These findings highlight EPSR5 as a potential candidate for the development of multi-targeted antidiabetic therapeutics derived from natural sources.

3.6. Assessment of antioxidant activity by TAC and FRAP

The total antioxidant capacity (TAC) of EPSR5 was evaluated using the phosphomolybdenum assay, which relies on the

Table 1 The antioxidant capacity and reducing power of EPSR5 expressed in ascorbic acid equivalents (AAE). Data is presented as mean ± SD, with $n = 3$ experiments

	TAC	FRAP
	Mean ± SE	Mean ± SE
EPSR5 (AAE) (μg mg^{-1})	62.8 ± 0.3	114.9 ± 0.5

reduction of molybdenum (Mo^{6+}) to Mo^{5+} by antioxidant compounds. This one-electron transfer reaction, conducted at acidic pH, results in the formation of a green-colored phosphate/Mo^{5+} complex, with the intensity of absorbance directly correlating to antioxidant capacity. EPSR5 demonstrated a TAC value of 62.8 ± 0.3 μg AAE per mg, as shown in Table 1, relative to the standard ascorbic acid control. These results suggest that EPSR5 has a strong electron-donating capacity, comparable to that of ascorbic acid. To further assess its antioxidant potential, EPSR5 was subjected to the ferric reducing antioxidant power (FRAP) assay. This method measures the ability of a compound to reduce Fe^{3+} to Fe^{2+}, which then forms a blue-colored Fe^{2+}–TPTZ complex in acidic conditions. The absorbance of this complex is directly proportional to the reducing power of the sample. EPSR5 exhibited a FRAP value of 114.9 ± 0.5 μg AAE per mg (Table 1), again comparable to the activity of ascorbic acid. Collectively, these results demonstrate that EPSR5 possesses considerable antioxidant properties through both total antioxidant capacity and ferric-reducing mechanisms. Its comparable performance to ascorbic acid in both assays indicates that EPSR5 could serve as a natural antioxidant agent with potential therapeutic applications.

3.7. Assessment of pancreatic lipase inhibition EPSR5

Pancreatic lipase is a key digestive enzyme responsible for hydrolyzing triglycerides into monoglycerides and free fatty acids. Inhibiting this enzyme reduces lipid absorption and overall cholesterol levels, making lipase inhibition a promising strategy for managing obesity and diabetes. The lipase inhibitory activity of EPSR5 was evaluated across a range of concentrations (1.95 to 1000 μg mL^{-1}) and compared to Orlistat, a clinically approved lipase inhibitor. As shown in Fig. 6, EPSR5 exhibited dose-dependent pancreatic lipase inhibition, reaching 90.1% inhibition at the highest tested concentration of 1000 μg mL^{-1}, compared to 96.9% inhibition by Orlistat. The IC_{50} value of EPSR5 was calculated as 41.39 μg mL^{-1}, whereas Orlistat showed a stronger inhibition with an IC_{50} of 13.79 μg mL^{-1}. These findings highlight EPSR5 as a potent pancreatic lipase inhibitor, demonstrating significant potential as a natural compound for managing lipid metabolism.

3.8. Assessment of wound healing activity *via* scratch assay

The wound healing or scratch assay is a well-established method for evaluating two-dimensional cell migration, serving as an *in vitro* model for tissue regeneration. In this study, EPSR5 exhibited a notably enhanced wound healing potential compared to untreated control cells. Wound closure was monitored at three time points: 0 h, 24 h, and 48 h. Initially (0 h), the mean wound area was comparable between the EPSR5-treated group (801.667 $μm^2$) and the control group (853 $μm^2$). After 48 hours, however, a substantial difference emerged: the EPSR5 group achieved a significant reduction in wound area to 225.667 $μm^2$, corresponding to a wound closure rate of 71.85%. In contrast, the control group showed a decrease to 288 $μm^2$, with a wound closure rate of 66.23% (Table 2 and Fig. 7). These results indicate that EPSR5 significantly enhances cell migration and promotes wound closure, suggesting its potential application in accelerating tissue repair and regeneration.

4. Discussion

Given the remarkable biomedical potential of exopolysaccharides and the ongoing search for novel marine-derived polymers, this study focused on EPSR5, an exopolysaccharide produced by the Red Sea isolate *Kocuria* sp. strain AG5 (Accession no. ON077051). In our earlier work, EPSR5 was shown to possess a relatively high molecular weight (4.9×10^4 g mol^{-1}) and an acidic nature, reflected in its sulfate (25.6%) and uronic acid (21.77%) contents. FTIR spectroscopy further confirmed the presence of characteristic polysaccharide

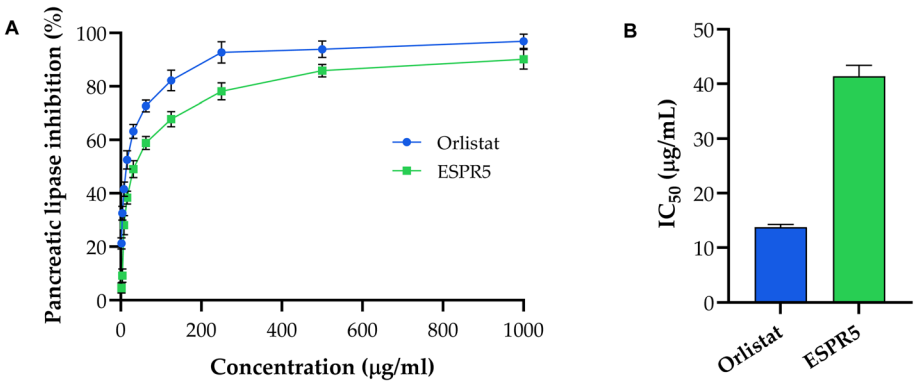

Fig. 6 The inhibitory activity of EPSR5 toward pancreatic lipase enzyme. (A and B) The dose-dependent inhibitory activity and IC_{50} value of EPSR5 as compared to orlistat toward pancreatic lipase. Data is presented as mean ± SD, with $n = 3$ experiments.

Table 2 Effect of EPSR5 on *in vitro* scratch assay wound closure over 48 hours

	At 0h		At 24h		At 48 h				
Item	Area, μm^2	Width, μm	Area, μm^2	Width, μm	Area, μm^2	Width, μm	RM, μm	Wound closure%, μm^2	Area difference, %
Control cells	867	866.037	777	776.165	301	300.167			
	751	750.131	725	724.011	297	296.007			
	861	860.114	740	738.531	377	376			
	843	842.059	695	694.012	343	342.286			
	885	884	721	720.225	253	252.032			
	911	910.02	827	826.01	157	156.115			
Mean	853	852.060	747.5	746.492	288	287.101	11.76998	66.23681	565
EPSR5	837	836.038	639	638.113	273	272.007			
(500 μg)	801	800.062	655	654.012	237	236.415			
	783	782.309	681	680.144	149	148.486			
	809	808.089	725	724.011	253	252.127			
	833	832.01	669	668.147	257	256.125			
	747	746.024	685	684.237	185	184.043			
Mean	801.667	800.755	675.667	674.777	225.667	224.867	11.99767	71.85031	576

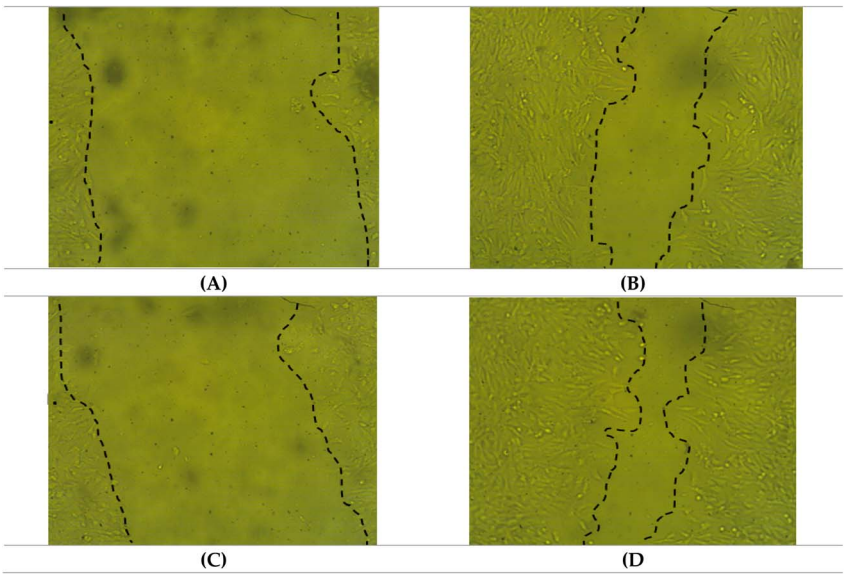

Fig. 7 Representative microscopic images illustrating wound closure during the *in vitro* scratch assay. (a) Control (untreated) cells at 0 h showing the initial wound area. (b) Control cells after 48 h demonstrated partial wound closure. (c) EPSR5-treated cells at 0 h showing the initial wound area. (d) EPSR5-treated cells after 48 h exhibited enhanced wound closure.

functional groups, including hydroxyl, carbonyl, and sulfate moieties, as well as pyranose ring signals, supporting its classification as an acidic heteropolysaccharide.[23] In the present study, we extended this characterization by employing complementary analytical platforms, GC–MS, HPLC, TGA, SEM, and EDX, to obtain a more comprehensive structural profile of EPSR5. The GC–MS analysis of derivatized hydrolysates revealed four monosaccharides: glucose, xylose, arabinose, and glucuronic acid, with arabinose detected in multiple silylated forms, a phenomenon commonly observed due to anomeric and ring configuration variations during derivatization. These findings were quantitatively validated by HPLC of PMP-derivatized hydrolysates,[43] which demonstrated glucose as the predominant monosaccharide (59.64%), followed by xylose (28.49%), with smaller contributions from glucuronic acid (7.37%) and arabinose (4.51%). The detection of glucuronic acid is particularly significant, as it reinforces the high uronic acid content previously determined by chemical assays and underlines the polyanionic, acidic character of EPSR5. The combined application of GC–MS and HPLC thus provided both qualitative and quantitative confirmation of the sugar composition, while ensuring consistency with earlier chemical and FTIR analyses. These results establish EPSR5 as a glucose-rich heteropolysaccharide with a polyanionic backbone, a structural feature commonly associated with the bioactivity of marine bacterial EPS. Such structural attributes, including the

presence of uronic acids, sulfate groups, and phosphorylation (as suggested by EDX), may collectively contribute to the diverse pharmacological effects observed in the biological assays presented in this work.[44,45] The TGA approach was employed to determine the heat resistance and decomposition behavior of EPSR5. The slight weight loss (258.8 mg of EPS) observed in the first stage of the TGA thermogram, from ambient temperature to 74.6 °C, was attributed to dehydration, specifically, the loss of physically bound water molecules associated with the carboxyl groups.[46] The second stage decomposition (139.8 °C) showed a weight loss of 54.0 mg of EPS, which is equivalent to thermally unstable functional group breakdown, which is the main cause of the weight loss during this phase. The third stage occurred between 257.07 °C and 644.46 °C, resulting in a weight loss of 70.7 mg. This mass reduction is attributed to the thermal degradation and depolymerization of the polysaccharide, involving the cleavage of C–C and C–O bonds in pyranose ring structures, leading to the release of H_2O and CO_2.[47] The residual mass observed at 644.46 °C indicated incomplete combustion. It can be concluded that the exopolysaccharide EPSR5 is thermostable up to 257.07 °C. This notable thermal stability may be attributed to the presence of uronic acids, which hinder complete polymer degradation. Specifically, galacturonic acid and xylose appear to play a role in influencing the pyrolysis process.[48] These findings demonstrate the potential suitability of EPSR5 for high-temperature industrial applications. The morphology and elemental content of the EPSR5 polymer were studied using SEM and EDX. The SEM analysis indicated that the EPSR5 appears to be irregularly shaped porous flakes with a smooth, glossy surface. Similarly, Xinyu *et al.* noted that the surface morphology of EPS extracted from *L. delbrueckii* subsp. *Bulgaricus* exhibited an unevenly porous surface distinguished by a stacked flake appearance.[49] Previous studies utilizing SEM indicated that EPS consisted of a homogeneous matrix characterized by either a smooth cubic surface or rough, irregular surfaces.[50] Furthermore, the energy-dispersive X-ray (EDX) spectra revealed the presence of oxygen, sodium, and phosphorus in EPSR5, with relatively high concentrations of oxygen (47.87%), sodium (25.34%), and phosphorus (26.79%). The phosphorylated nature of EPSR5 suggests enhanced bioactivity, indicating its potential as an immunomodulator or as a candidate for the development of autoimmune therapies.[51] The relatively high sodium content detected can be attributed to the strong association of sodium ions with the anionic functional groups of EPSR5, particularly its uronic acid (21.77%) and sulfate (25.6%) moieties. These negatively charged groups require counter-ions for charge neutrality, and sodium likely remains bound to the EPS structure. Similar sodium enrichment has been reported for other marine bacterial exopolysaccharides, where it plays a stabilizing role in the polymeric matrix.[52]

It is well established that polysaccharides, owing to their negatively charged sulfate and uronic acid groups, interact effectively with Gram-positive bacteria, which have more positively charged cell walls. Additionally, the molecular weight of polysaccharides plays a significant role in their activity by enabling the formation of a physical barrier that inhibits bacterial growth and colonization.[53] In the current study, the antimicrobial activity of EPSR5 was evaluated against seven ATCC pathogenic microbes, including two fungal strains, two Gram-positive bacteria, and three Gram-negative bacteria. EPSR5 demonstrated potent activity against select Gram-positive and Gram-negative bacteria, as well as fungal strains. Among Gram-positive bacteria, EPSR5 showed the strongest inhibition against *Enterococcus faecalis*, with a 30 mm inhibition zone compared to 24 mm for gentamicin; the corresponding MIC and MBC values were 7.8 and 15.62 μg mL^{-1}, respectively. Against Gram-negative bacteria, EPSR5 exhibited superior antibacterial activity against *Helicobacter pylori*, producing a 27 mm inhibition zone *versus* 21 mm for gentamicin, with MIC and MBC values both at 15.62 μg mL^{-1}. Additionally, EPSR5 yielded a 28 mm inhibition zone against *Escherichia coli*, compared to 21 mm for gentamicin, with MIC and MBC values of 15.62 and 62.5 μg mL^{-1}, respectively. For the fungal strain *Candida albicans*, EPSR5 produced a 27 mm clearance zone *versus* 24 mm for fluconazole, with MIC and MFC values of 62.5 and 250 μg mL^{-1}, respectively. Supporting our findings, a study by Aullybux *et al.* reported the extraction of eight EPS with antibacterial properties against a wide range of microbial pathogens, including *Bacillus*, *Halomonas*, *Psychrobacter*, and *Alcaligenes* species. Among these, certain EPS exhibited the most potent activity, with MIC values ranging from 62.5 to 500 μg mL^{-1}. The study suggested that the presence of curdlan, levan, and sulfate groups in the identified EPS contributes significantly to their antimicrobial effects against diverse pathogens.[54] Several studies have shown that bacterial EPS possess significant antimicrobial activity against various pathogens, acting through multiple mechanisms such as disrupting cell division, compromising cell wall and membrane integrity, damaging DNA, and interfering with respiratory chains and other key metabolic pathways.[30,55] Biofilms are microbial colonies that attach to surfaces and consist of bacterial cells wrapped in a self-synthetic polymer matrix.[56] In the current study, the antibiofilm efficacy of EPSR5 was evaluated against Gram-positive bacteria (*E. faecalis* and *Staphylococcus aureus*) and Gram-negative bacteria (*H. pylori* and *E. coli*). Among the Gram-positive strains, *E. faecalis* showed the highest inhibition rates of 96.54%, 94.18%, and 92.61% at 75%, 50%, and 25% of the MBC, respectively. For Gram-negative bacteria, *H. pylori* exhibited the strongest antibiofilm activity with 97.39% inhibition at 75% MBC and 91.89% at 25% MBC. These results highlight the potent, dose-dependent antibiofilm activity of EPSR5, particularly against *E. faecalis* and *H. pylori*. Notably, even at half and one-quarter of the MBC, EPSR5 maintained significant inhibition, indicating sustained efficacy at lower concentrations. In alignment with our findings, a study reported that sulfated exopolysaccharide from *Bacillus licheniformis* LHG166 exhibited strong antibiofilm activity, achieving 96.63% inhibition against *E. coli*, followed by 86.91% against *S. typhi*, 86.45% against *P. aeruginosa*, and 84.36% against *K. pneumoniae*.[57]

Next, the antioxidant capacity of EPSR5 was evaluated using TAC and FRAP assays. The TAC value was 62.8 ± 0.3 μg AAE per mg, while the FRAP value was 114.9 ± 0.5 μg AAE per mg,

confirming its notable antioxidant potential. Chemical analysis of EPS revealed distinct monosaccharides in varying ratios, classified as reducing sugars due to the presence of aldoses, ketoses, or their ability to interconvert. These monosaccharides possess aldehyde groups, making them effective reducing agents.[58,59] EPS antioxidant activity is influenced by factors such as monosaccharide composition, molecular weight, and functional groups, which contribute to reducing oxidative stress by scavenging free radicals, preventing lipid peroxidation, and donating electrons or protons.[60] Several reports have demonstrated the antioxidant potential of EPS derived from probiotic bacteria, showing activity through superoxide and hydrogen peroxide scavenging, ROS reduction, and metal chelation.[61] Diabetes mellitus is a metabolic disorder characterized by elevated blood glucose levels due to improper glucose metabolism, which causes numerous organ failures.[61] Acarbose and other anti-diabetic medicines induce stomach distension, bowel disturbance, and diarrhea, making them inappropriate for people with gastrointestinal diseases.[59] Our study suggests that microbial EPSR5 exhibits inhibitory potential against α-amylase and α-glucosidase, which was relative to acarbose, indicating its antidiabetic activity. These findings indicate that EPSR5 may inhibit hydrolysis *via* binding to the active site of enzymes or substrates.[58,59] On the other hand, pancreatic lipase is the primary enzyme that degrades dietary lipids and its inhibition offers several advantages for managing diabetes by reducing fat absorption, stabilizing postprandial blood glucose levels, and enhancing insulin sensitivity.[62,63] Our study demonstrated that EPSR5 inhibited lipase activity, with an IC_{50} of 41.39 μg mL^{-1} compared to Orlistat's IC_{50} of 13.79 μg mL^{-1}. At 1000 μg mL^{-1}, EPSR5 suppressed lipase activity by 90.1%, while Orlistat achieved 96.9% inhibition. These findings suggest that EPSR5 has the potential to help reduce high cholesterol levels if incorporated into functional foods. Supporting our findings, a study reported that probiotic strains lower cholesterol through multiple mechanisms, including bacterial cell expansion reducing cholesterol absorption, bile salt deconjugation by bile salt hydrolase, cholesterol deposition with deconjugated bile, and direct cholesterol binding to bacterial cells.[64] The wound healing scratch assay is a simple *in vitro* method to study fibroblast migration, a key process in skin repair. Understanding how materials affect this migration can help develop targeted treatments for improved wound healing.[65,66] The scratch assay demonstrated that EPSR5 significantly enhanced wound healing compared to the control. Treatment with EPSR5 reduced the wound area from an average of 801.67 μm^2 to 225.67 μm^2 within two days, achieving 71.85% closure. In contrast, the control group showed 66.24% closure, with the wound area decreasing from 853 μm^2 to 288 μm^2. Cell migration data demonstrate EPSR5's ability to promote proliferation and migration, highlighting its strong bioactivity and potential for medical applications in wound healing. Peptic ulcers, commonly caused by *H. pylori* infection, result from disruption of the gastric mucosal barrier and require effective tissue repair.[67] The ability of EPSR5 to enhance cell migration and proliferation may accelerate gastric lining repair, promoting faster healing of ulcers. Additionally, its bio-responsive properties could help modulate the local immune response, supporting recovery from *H. pylori*-induced gastric damage. Together, EPSR5 demonstrated strong antibacterial, antifungal, and biofilm-inhibiting activities, along with notable antioxidant and antidiabetic effects through enzyme inhibition. It also promoted wound healing by enhancing fibroblast migration and closure rates, indicating therapeutic potential for wound care and peptic ulcer treatment. These multifaceted bioactivities position EPSR5 as a promising candidate for advanced pharmacological applications.

5. Conclusion

In conclusion, the present study provides a comprehensive structural and pharmacological evaluation of EPSR5, a marine-derived exopolysaccharide isolated from *Kocuria* sp. AG5. The structural analysis confirmed the presence of α-pyranoside linkages and characteristic functional groups typical of bioactive polysaccharides, while TGA demonstrated stability up to 257 °C. Morphological and elemental characterization *via* SEM and EDX revealed a porous, flake-like structure enriched with oxygen, sodium, and phosphorus, indicating potential phosphorylation that may enhance its biological activity. EPSR5 displayed robust pharmacological properties across several biomedical assays. EPSR5 demonstrated potent and broad-spectrum antimicrobial activity against clinically relevant bacterial and fungal strains, including multidrug-resistant pathogens. Its ability to inhibit biofilm formation at sub-MBC concentrations underscores its potential as an anti-virulence agent. In addition to its antimicrobial effects, EPSR5 showed significant antioxidant capacity, pancreatic lipase inhibition, and dual antidiabetic activity through α-amylase and α-glucosidase inhibition, comparable to or approaching standard drugs like Acarbose and Orlistat. Furthermore, EPSR5 significantly enhanced fibroblast migration and wound closure *in vitro*, indicating its promise in wound healing and tissue regeneration. Overall, the multifunctional bioactivities of EPSR5 demonstrate its broad therapeutic promise. These findings not only expand the current knowledge of marine bacterial exopolysaccharides but also support the potential development of EPSR5 as a novel natural therapeutic agent for a variety of clinical and pharmaceutical applications. Future work should focus on elucidating the precise molecular mechanisms of action, conducting *in vivo* efficacy and toxicity assessments, and exploring formulation strategies for potential biomedical and nutraceutical products.

Author contributions

Conceptualization, MMG, RAA, AG, SZA, AAA, and HFA; methodology, MMG, RAA, AG, MMH, SMA, HA, FMKA, FOA, SAA, SZA, AAA, and HFA; software, MMG, AG, MMH, SMA, HA, FMKA, FOA, SAA, and HFA; validation, MMG, AG, MMH, HA, FMKA, FOA, SAA, SZA, and HFA; formal analysis, MMG, AG, MMH, SMA, FMKA, FOA, SAA, SZA, and HFA; investigation, MMG, RAA, AG, HA, FMKA, FOA, SAA, AAA, and HFA; resources, MMG, AG, MMH, HA, FOA, SAA, AAA, and HFA; data curation,

RAA., AG, HA, FMKA, FOA, SAA, SZA, and HFA; writing—original draft preparation MMG, RAA, AG, MMH, SMA, HA, FMKA, FOA, SAA, SZA, AAA, and HFA; writing—review and editing, MMG, RAA, AG, MMH, SMA, HA, FMKA, FOA, SAA, SZA, AAA, and HFA; visualization, MMG, RAA, MMH, SMA, HA, FOA, SZA, and HFA; supervision, RAA, AG, HA, SAA, AAA, and HFA; project administration, MMG, RAA, AG, SZA, AAA, and HFA; funding acquisition, MMG, RAA, SZA, AAA, and HFA. All authors have read and agreed to the published version of the manuscript.

Conflicts of interest

The authors affirm that they are not aware of any personal or financial conflicts that would have seemed to affect the findings of this study's research.

Data availability

Data supporting the results reported in this manuscript are included in this article and as part of the SI. The raw data supporting the conclusions of this article will be made available by the authors without any undue reservation. Samples of final compounds are available by the authors upon request.

Acknowledgements

The authors acknowledge Princess Nourah Bint Abdulrahman University for funding this work through the Researchers Supporting Project number (PNURSP2025R488), Princess Nourah Bint Abdulrahman University, Riyadh, Saudi Arabia.

References

1 A. Poli, I. Finore, I. Romano, A. Gioiello, L. Lama and B. Nicolaus, *Microorganisms*, 2017, **5**, 25.
2 A. M. G. Darwish, N. M. Abdelmotilib, A. M. Abdel-Azeem, H. H. Abo Nahas and M. T. Mohesien, in *Recent Developments on Genus Chaetomium*, ed. A. M. Abdel-Azeem, Springer International Publishing, Cham, 2020, pp. 227–240.
3 F. Benhadda, A. Zykwinska, S. Colliec-Jouault, C. Sinquin, B. Thollas, A. Courtois, N. Fuzzati, A. Toribio and C. Delbarre-Ladrat, *Mar. Drugs*, 2023, **21**, 582.
4 S. A. M. Khalifa, N. Elias, M. A. Farag, L. Chen, A. Saeed, M.-E. F. Hegazy, M. S. Moustafa, A. Abd El-Wahed, S. M. Al-Mousawi, S. G. Musharraf, F.-R. Chang, A. Iwasaki, K. Suenaga, M. Alajlani, U. Göransson and H. R. El-Seedi, *Mar. Drugs*, 2019, **17**, 491.
5 A. M. S. Mayer, V. A. Mayer, M. Swanson-Mungerson, M. L. Pierce, A. D. Rodríguez, F. Nakamura and O. Taglialatela-Scafati, *Mar. Drugs*, 2024, **22**, 309.
6 N. Barzkar, S. Sukhikh and O. Babich, *Front. Microbiol.*, 2024, **14**, 1285902.
7 A. I. Netrusov, E. V. Liyaskina, I. V. Kurgaeva, A. U. Liyaskina, G. Yang and V. V. Revin, *Microorganisms*, 2023, **11**, 1541.
8 S. Carillo, A. Casillo, G. Pieretti, E. Parrilli, F. Sannino, M. Bayer-Giraldi, S. Cosconati, E. Novellino, M. Ewert, J. W. Deming, R. Lanzetta, G. Marino, M. Parrilli, A. Randazzo, M. L. Tutino and M. M. Corsaro, *J. Am. Chem. Soc.*, 2015, **137**, 179–189.
9 P. Laurienzo, *Mar. Drugs*, 2010, **8**, 2435–2465.
10 T. Le Costaouëc, S. Cérantola, D. Ropartz, J. Ratiskol, C. Sinquin, S. Colliec-Jouault and C. Boisset, *Carbohydr. Polym.*, 2012, **90**, 49–59.
11 M.-L. Sun, F. Zhao, M. Shi, X.-Y. Zhang, B.-C. Zhou, Y.-Z. Zhang and X.-L. Chen, *Sci. Rep.*, 2015, **5**, 18435.
12 H. Yildiz and N. Karatas, *Process Biochem.*, 2018, **72**, 41–46.
13 X. Sun and J. Zhang, *Int. J. Biol. Macromol.*, 2021, **173**, 481–490.
14 J. Wang, J. Chen, S. Ye, D. Zhang, Y. Cui and Y. Ding, *J. Mol. Struct.*, 2023, **1294**, 136402.
15 M. Qi, C. Zheng, W. Wu, G. Yu and P. Wang, *Mar. Drugs*, 2022, **20**, 512.
16 A. Poli, G. Anzelmo and B. Nicolaus, *Mar. Drugs*, 2010, **8**, 1779–1802.
17 W. Chaisuwan, K. Jantanasakulwong, S. Wangtueai, Y. Phimolsiripol, T. Chaiyaso, C. Techapun, S. Phongthai, S. You, J. M. Regenstein and P. Seesuriyachan, *Food Biosci.*, 2020, **35**, 100564.
18 P. Stincone and A. Brandelli, *Crit. Rev. Biotechnol.*, 2020, **40**, 306–319.
19 B. Almutairi and M. Helal, *J. King Saud Univ., Sci.*, 2020, **33**, 101328.
20 A. K. Abdalla, M. M. Ayyash, A. N. Olaimat, T. M. Osaili, A. A. Al-Nabulsi, N. P. Shah and R. Holley, *Front. Microbiol.*, 2021, **12**, 664395.
21 D. Rubini, P. Varthan, J. Senthilganesh, B. Vedahari and P. Nithyanand, *Microb. Pathog.*, 2020, **141**, 103973.
22 S. Wu, G. Liu, W. Jin, P. Xiu and C. Sun, *Front. Microbiol.*, 2016, **7**, 102.
23 S. Z. Alshawwa, K. S. Alshallash, A. Ghareeb, A. M. Elazzazy, M. Sharaf, A. Alharthi, F. E. Abdelgawad, D. El-Hossary, M. Jaremko, A.-H. Emwas and Y. A. Helmy, *Life*, 2022, **12**, 1387.
24 M. Sharar, E. M. Saied, M. C. Rodriguez, C. Arenz, M. Montes-Bayón and M. W. Linscheid, *Anal. Bioanal. Chem.*, 2017, **409**, 2015–2027.
25 M. U. Kakar, J. Li, M. Z. Mehboob, R. Sami, N. Benajiba, A. Ahmed, A. Nazir, Y. Deng, B. Li and R. Dai, *Sci. Rep.*, 2022, **12**, 8160.
26 M. S. Refat, H. K. Ibrahim, S. Z. A. Sowellim, M. H. Soliman and E. M. Saied, *J. Inorg. Organomet. Polym. Mater.*, 2014, **24**, 904.
27 D. I. Mohamed, S. F. Ezzat, W. M. Elayat, O. A. El-Kharashi, H. F. A. El-Kareem, H. H. A. Nahas, B. A. Abdel-Wahab, S. Z. Alshawwa, A. Saleh, Y. A. Helmy, E. Khairy and E. M. Saied, *Pharmaceuticals*, 2022, **15**, 832.
28 S. Magaldi, S. Mata-Essayag, C. Hartung de Capriles, C. Perez, M. T. Colella, C. Olaizola and Y. Ontiveros, *Int. J. Infect. Dis.*, 2004, **8**, 39–45.
29 S. Koch-Edelmann, S. Banhart, E. M. Saied, L. Rose, L. Aeberhard, M. Laue, J. Doellinger, C. Arenz and D. Heuer, *Cell. Microbiol.*, 2017, **19**, e12752.

30 M. M. Labib, A. M. Alqahtani, H. H. Abo Nahas, R. M. Aldossari, B. F. Almiman, S. Ayman Alnumaani, M. El-Nablaway, E. Al-Olayan, M. Alsunbul and E. M. Saied, *Biomolecules*, 2024, **14**, 1018.
31 A. Malm, A. Glowniak-Lipa, I. Korona-Glowniak and T. Baj, *Curr. Issues Pharm. Med. Sci.*, 2015, **28**, 30–32.
32 A. Espinel-Ingroff, *J. Clin. Microbiol.*, 2001, **39**, 954–958.
33 A. L. S. Antunes, D. S. Trentin, J. W. Bonfanti, C. C. F. Pinto, L. R. R. Perez, A. J. Macedo and A. L. Barth, *APMIS*, 2010, **118**, 873–877.
34 M. N. Wickramaratne, J. C. Punchihewa and D. B. M. Wickramaratne, *BMC Complementary Altern. Med.*, 2016, **16**, 466.
35 G. Pistia-Brueggeman and R. I. Hollingsworth, *Tetrahedron*, 2001, **57**, 8773–8778.
36 S. M. Khirallah, H. M. M. Ramadan, H. A. A. Aladl, N. O. Ayaz, L. A. F. Kurdi, M. Jaremko, S. Z. Alshawwa and E. M. Saied, *Pharmaceuticals*, 2022, **15**, 1576.
37 P. Prieto, M. Pineda and M. Aguilar, *Anal. Biochem.*, 1999, **269**, 337–341.
38 I. Lahmass, S. Ouahhoud, M. Elmansuri, A. Sabouni, M. Elyoubi, R. Benabbas, M. Choukri and E. Saalaoui, *Waste Biomass Valorization*, 2018, **9**, 1349–1357.
39 I. F. F. Benzie and J. J. Strain, *Anal. Biochem.*, 1996, **239**, 70–76.
40 S. Athamena, S. Laroui, W. Bouzid and A. Meziti, *J. Herbs, Spices Med. Plants*, 2019, **25**, 271–286.
41 Y. S. Kim, Y. M. Lee, H. Kim, J. Kim, D. S. Jang, J. H. Kim and J. S. Kim, *J. Ethnopharmacol.*, 2010, **130**, 621–624.
42 V. Rötzer, E. Hartlieb, J. Winkler, E. Walter, A. Schlipp, M. Sardy, V. Spindler and J. Waschke, *J. Invest. Dermatol.*, 2016, **136**, 301–310.
43 C. Bailly, P.-E. Hecquet, M. Kouach, X. Thuru and J.-F. Goossens, *Bioorg. Med. Chem.*, 2020, **28**, 115463.
44 M. Qi, C. Zheng, W. Wu, G. Yu and P. Wang, *Mar. Drugs*, 2022, **20**, 512.
45 W. Wang, Y. Ju, N. Liu, S. Shi and L. Hao, *Chem. Biol. Technol. Agric.*, 2023, **10**, 137.
46 K. Yelithao, U. Surayot, W. Park, S. Lee, D.-H. Lee and S. You, *Int. J. Biol. Macromol.*, 2019, **122**, 10–18.
47 M. H. Saad, N. M. Sidkey and E. M. El-Fakharany, *Microb. Cell Factories*, 2024, **23**, 117.
48 H. Wang, H. Hu, Y. Yang, H. Liu, H. Tang, S. Xu, A. Li and H. Yao, *Waste Manage.*, 2020, **118**, 9–17.
49 G. Xinyu, M. Fengming and Z. Baiqing, *Int. J. Food Sci. Technol.*, 2021, **56**, 865–873.
50 E. H. Zaghloul and M. I. A. Ibrahim, *Front. Microbiol.*, 2022, **13**, 903363.
51 T. A. Olasehinde, L. V. Mabinya, A. O. Olaniran and A. I. Okoh, *Int. J. Food Prop.*, 2019, **22**, 100–110.
52 A. Casillo, R. Lanzetta, M. Parrilli and M. M. Corsaro, *Mar. Drugs*, 2018, **16**, 69.
53 A. K. Abdalla, M. M. Ayyash, A. N. Olaimat, T. M. Osaili, A. A. Al-Nabulsi, N. P. Shah and R. Holley, *Front. Microbiol.*, 2021, **12**, 664395.
54 A. A. Aullybux, D. Puchooa, T. Bahorun and R. Jeewon, *Ann. Microbiol.*, 2019, **69**, 957–972.
55 M.-H. Wu, T.-M. Pan, Y.-J. Wu, S.-J. Chang, M.-S. Chang and C.-Y. Hu, *Int. J. Food Microbiol.*, 2010, **144**, 104–110.
56 S. Sharma, J. Mohler, S. D. Mahajan, S. A. Schwartz, L. Bruggemann and R. Aalinkeel, *Microorganisms*, 2023, **11**, 1614.
57 N. K. Alharbi, Z. F. Azeez, H. M. Alhussain, A. M. A. Shahlol, M. O. I. Albureikan, M. G. Elsehrawy, G. S. Aloraini, M. El-Nablaway, E. M. Khatrawi and A. Ghareeb, *Front. Microbiol.*, 2024, **15**, 1385493.
58 M. A. Alharbi, A. M. A. Shahlol, M. O. I. Albureikan, K. Johani, M. G. Elsehrawy, M. El-Nablaway, F. M. Saleh, A. F. Basyony, S. A. Zakai and A. Ghareeb, *Arch. Med. Sci.*, 2024, 190065.
59 G. S. Aloraini, M. O. I. Albureikan, A. M. A. Shahlol, T. Shamrani, H. Daghistani, M. El-Nablaway, N. A. Tharwat, A. M. Elazzazy, A. F. Basyony and A. Ghareeb, *Rev. Adv. Mater. Sci.*, 2024, **63**(1), 20240016.
60 B. A. Abdel-Wahab, H. F Abd El-Kareem, A. Alzamami, C. A Fahmy, B. H Elesawy, M. Mostafa Mahmoud, A. Ghareeb, A. El Askary, H. H. Abo Nahas, N. G M Attallah, N. Altwaijry and E. M Saied, *Metabolites*, 2022, **12**, 715.
61 J. Angelin and M. Kavitha, *Int. J. Biol. Macromol.*, 2020, **162**, 853–865.
62 N. A. Lunagariya, N. K. Patel, S. C. Jagtap and K. K. Bhutani, *EXCLI J.*, 2014, **13**, 897–921.
63 A. Kumar and S. Chauhan, *Life Sci.*, 2021, **271**, 119115.
64 M. Kumar, R. Nagpal, R. Kumar, R. Hemalatha, V. Verma, A. Kumar, C. Chakraborty, B. Singh, F. Marotta, S. Jain and H. Yadav, *J. Diabetes Res.*, 2012, **2012**, 902917.
65 X. Alvarez, A. Alves, M. P. Ribeiro, M. Lazzari, P. Coutinho and A. Otero, *Carbohydr. Polym.*, 2021, **254**, 117303.
66 C.-C. Liang, A. Y. Park and J.-L. Guan, *Nat. Protoc.*, 2007, **2**, 329–333.
67 D. Majumdar and S. Looi, *Medicine*, 2024, **52**, 152–160.